Desalination and Water Treatment
www.deswater.com
doi: 10.1080/19443994.2015.1029009

57 (2016) 7627–7636
April

Taylor & Francis
Taylor & Francis Group

Development of a nanofiltration membrane for humic acid removal through the formation of polyelectrolyte multilayers that contain nanoparticles

Law Yong Ng[a], Abdul Wahab Mohammad[b,c,*], Rosiah Rohani[b], Nur Hanis Hayati Hairom[b]

[a]*Universiti Kuala Lumpur International College, Malaysian Institute of Chemical & Bioengineering Technology, Universiti Kuala Lumpur, Lot 1988 Bandar Vendor, Taboh Naning, 78000 Alor Gajah, Melaka, Malaysia, Tel. +6017 2102294; email: nglawyong@gmail.com*
[b]*Faculty of Engineering and Built Environment, Department of Chemical and Process Engineering, 43600 UKM Bangi, Selangor, Malaysia, Tel. +603 8921 6410; Fax: +603 8921 6148; email: wahabm@eng.ukm.my (A.W. Mohammad); Tel. +603 89216408; email: rosiah@eng.ukm.my (R. Rohani), Tel. +019 3836454; email: nurhanishayati@gmail.com (N.H.H. Hairom)*
[c]*Research Centre for Sustainable Process Technology (CESPRO), Universiti Kebangsaan Malaysia, 43600 UKM Bangi, Selangor, Malaysia*

Received 24 December 2014; Accepted 9 March 2015

ABSTRACT

Poly(sodium-4-styrenesulphonate) (PSS) and poly(diallyldimethylammonium chloride) have been employed to construct polyelectrolyte multilayers on a polyethersulphone substrate for use in the nanofiltration of humic acid. Self-synthesised Ag_2O and commercial ZnO nanoparticles were incorporated into the multilayers separately, showing increases in the permeability from 7.53 ± 1.83 to 8.39 ± 1.37 and 8.62 ± 1.03 $L\,m^{-2}\,h^{-1}\,bar^{-1}$, respectively, with no significant leaching observed in the permeates. All polyelectrolyte-modified membranes exhibited good film-formation stabilities and high humic acid retention capabilities, which ranged from 93.14 ± 2.43 to 95.57 ± 3.87%. Less humic acid solutes were deposited onto the surface of the polyelectrolyte-modified membrane, which was confirmed through field emission scanning electron microscopy images. The contact angle was reduced from 44.00 ± 3.46° to 39.10 ± 3.47° when the membrane surface was hydrophilised with PSS as the terminating layer.

Keywords: Nanoparticles; Self-assembly; Nanofiltration; Polyelectrolytes; Humic acid; Selectivity

1. Introduction

Natural organic matter (NOM) has been recognised as one of the main foulants present in surface water and wastewater, which could affect the performance of membrane filtration systems [1]. Its presence in potable water filtration systems can also contribute to the formation of hazardous materials such as trihalomethanes [2]. Nanofiltration (NF) is the preferred process for the partial removal of NOM and divalent

---

*Corresponding author.

Presented at the 7th International Conference on Challenges in Environmental Science and Engineering (CESE 2014) 12–16 October 2014, Johor Bahru, Malaysia

1944-3994/1944-3986 © 2015 Balaban Desalination Publications. All rights reserved.

salts from water filtration systems [3], owing to its moderate operating pressure and effective performance, as it involves a combination of size exclusion and the Donnan effect [4]. Deposition of organic materials such as NOM onto a membrane surface is favoured, because of hydrophobic interactions between the solutes and the membrane surface [5], which will reduce the number of open membrane pores, thus minimising the membrane solution flux and lifespan. This phenomenon can be minimised through membrane surface modification, which enhances the membrane surface hydrophilicity and solute retention capability.

Inorganic nanoparticles have previously been studied in terms of their outstanding properties, such as antimicrobial properties [6,7], owing to their high surface-area-to-volume ratios. This has encouraged the incorporation of nanoparticles into fabrics, polymers, and composites [8] for wider applications. Nanoparticles have also been studied for water treatment processes, which normally involve water filtration membranes [9,10]. Many types of nanoparticles have previously been studied, including silver bromide, silver chloride, zinc oxide [11], and so forth, to improve membrane effectiveness in preventing biofouling [12].

Inorganic nanoparticles can vary membrane properties through the blending method, but this method requires an excessive amount of nanoparticles to be distributed over the whole membrane matrix, which causes a higher nanoparticle leaching rate [13]. In fact, incorporation of nanoparticles onto the membrane surface alone is sufficient to provide the membrane with the desired properties, especially antimicrobial activity, because of its direct impact on the micro-organism through the long-lasting contact time [13] and it requires a lower amount of nanoparticles, thus reducing production costs. However, challenges still need to be overcome in terms of incorporation methods and finding appropriate materials. Thus, this is the subject of the current study.

Poly(sodium-4-styrenesulphonate) (PSS) and poly (diallyldimethylammonium chloride) (PDADMAC) multilayers are suggested in this work to incorporate inorganic nanoparticles into a polyethersulphone (PES) membrane surface through static deposition. Polyelectrolytes with high charge densities have been suggested to be used as “electrostatic glue” for the assembly of colloidal nanoparticles [14], forming a tight complex and, therefore, a better separation capability in an environmentally friendly way. It offers selective ion transport, originating from the multibipolar structure of the separating membrane; thus, rejection of multivalent ions is expected to be higher. This work also observed the distributions of inorganic nanoparticles in polyelectrolyte multilayers through energy dispersive X-ray analysis, which was carried out in mapping mode. Stability of the polyelectrolyte multilayers is an important aspect in membrane applications, but is often neglected. Thus, this work also studied the leaching behaviours of nanoparticle and polyelectrolyte-modified membranes through inductively coupled plasma (ICP) and UV absorbance analyses.

2. Materials and methods

2.1. Materials

NF1 (a commercial PES NF membrane, with an $MgSO_4$ retention of approximately 98% when using a solution of 2,000 mg/L at 10.34 bar and 25˚C through pilot-plant testing) and PES20 (a commercial PES ultrafiltration (UF) membrane with a nominal molecular weight cut-off of 20,000 g mol^{-1}) were purchased from Amfor Inc., China. PSS and PDADMAC solutions, with an average molecular weight of 1,000,000 and 400,000–500,000 g mol^{-1}, respectively, were purchased from Sigma-Aldrich. Humic acid, polyethylene glycol (PEG), and ZnO nanoparticles (50–140 nm) were supplied by Sigma-Aldrich. NaOH, NaCl, $AgNO_3$, Na_2SO_4, and $MgSO_4$ were purchased from Merck and used without further purification. Ag_2O nanoparticles were prepared by adapting a previously reported method, using PEG as a reducing and stabilising agent [8]. PEG solution was used to facilitate the reduction reaction and to prevent agglomeration of the nanoparticles [8].

2.2. Membrane modification method

Low thermal treatment at 50˚C was employed on commercial PES20 membranes [15] for 17.07 min, using a forced-air convection oven (Froilabo, France) to avoid membrane degradation, which was followed by the deposition of PDADMAC/PSS layers [16,17]. PSS solution was combined with 0.1 wt% of the nanoparticles to minimise the effect of agglomeration [18] and to produce polyelectrolyte layers containing the nanoparticles (see Table 1).

2.3. Analysis of the water permeability

The membrane water flux (J) was determined by reverse osmosis with water at room temperature using a Sterlitech HP4750 stirred cell and calculations using Eq. (1) [19], in which V is the volume of water (L), S is the membrane surface area (m^2), and t is the time interval (h). ICP analyses were conducted on the

Table 1
Membrane label description and associated water permeability

Membrane label	Base membrane	Modification	Water permeability ($L\ m^{-2}\ h^{-1}\ bar^{-1}$)
A	NF1	Unmodified membrane	7.90 ± 2.39
B	PES20	Unmodified membrane	135.23 ± 7.64
C	PES20	2 bilayers of PDADMAC/PSS	7.53 ± 1.83
D	PES20	2 bilayers of PDADMAC/PSS. PSS layers were incorporated with Ag_2O nanoparticles	8.39 ± 1.37
E	PES20	2 bilayers of PDADMAC/PSS. PSS layers were incorporated with ZnO nanoparticles	8.62 ± 1.03

samples collected from the retentate and permeate (for Membrane D and Membrane E, respectively) in order to observe the leaching behaviours.

$$J = V/(S \times t) \tag{1}$$

2.4. Solute-retention analysis

NaCl, $MgSO_4$, and Na_2SO_4 single-salt solutions (100 ppm each) and humic acid solution (10 ppm) were used for solute retention analysis. In fact, mixed-salt solutions can provide higher salt retention results and require a minimal number of experimental runs compared to single-salt solutions [20], but complications then accrue in determining the membrane rejection or selectivity towards each single salt in the mixed-salt solution [16]. Thus, the current work employed single-salt solutions for all retention analyses. A stirring rate of 1,000 rpm was employed during the permeation test at 5 bar in order to collect about 100 mL of the permeated samples, but the stirring effect is neglected [21] and not explored further. The salt and humic acid permeate concentrations (C_p) were determined using electrical conductivity measurements [21] and UV absorbance analyses at a wavelength of 254 nm [22], respectively. The retention percentages ($R_{obs}\%$) were calculated using Eq. (2) [19], in which C_f is the feed concentration:

$$R_{obs}\% = (1 - C_p/C_f) \times 100\% \tag{2}$$

2.5. Nanoparticle and membrane characterisation

The X-ray diffraction (XRD) pattern of the self-synthesised Ag_2O particles was analysed using a Bruker D8 Advance Instrument (Germany). A transmission electron microscope (CM 12 Philips model, Netherlands) was used to image and measure the sizes of the nanoparticles. A Nano series Zetasizer instrument was employed to obtain the size distributions of the nanoparticles in order to describe the sizes of the nanoparticles in bulk quantities. The membrane surfaces were examined using a field emission scanning electron microscope (Gemini model SUPRA 55VP-ZEISS). In addition, energy dispersive X-ray (EDX) elemental analyses were conducted in mapping mode, using an INCA instrument (supplied by Oxford) to investigate the dispersion patterns of nanoparticles in the polyelectrolyte multilayers. Membrane surface contact angles were measured using a Drop Shape Analysis System goniometer (model DSA100, Kruss GmbH, Germany), as described elsewhere [19]. UV absorbance measurements were conducted on the samples collected from permeates and retentates. Traces of polyelectrolytes were then evaluated.

3. Results and discussion

3.1. Zeta potential and size distribution analyses of the nanoparticles

XRD results confirmed that Ag_2O nanoparticles were successfully synthesised with high crystallinity, and traces of pure silver nanoparticles (approximately 2.3%) were also present in the samples (Fig. 1). Similar XRD patterns for silver and silver oxide have been reported elsewhere [23]. The approximate sizes of the Ag_2O and ZnO nanoparticles, obtained by direct measurements using a TEM device and computational software, were <20 nm. Size distribution analysis using a dynamic light scattering process measured the Brownian motion and related this to the size of the particles by illuminating the particles with a laser and then analysing the intensity fluctuations in the scattered light. The average agglomerate sizes of the Ag_2O and ZnO nanoparticles were measured as 76.38 and 195 nm, respectively. Dispersions of the nanoparticles are dependent on nanoparticle surface charges. When the surface charge density is high, nanoparticles possess the capability to repel particles in their surroundings

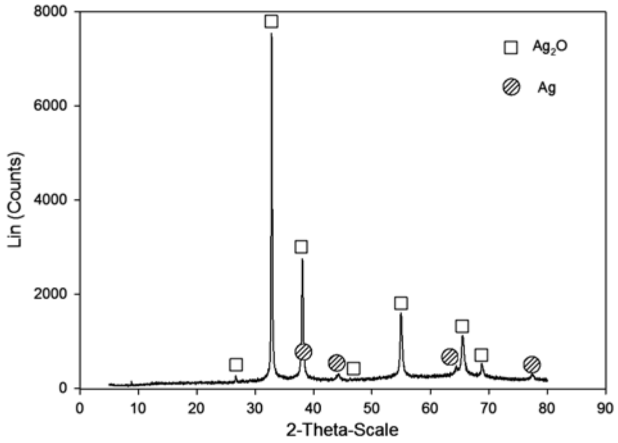

Fig. 1. XRD analysis for silver oxide nanoparticles.

with that same charge, thus minimising agglomeration. Zeta potential measurements showed that Ag_2O nanoparticles exhibit an average zeta potential value of –32.9 mV, which makes the Ag_2O nanoparticles more negatively charged than ZnO nanoparticles (–1.86 mV).

3.2. *Dispersion of nanoparticles within polyelectrolyte multilayers*

Fig. 2(a) and (b) verifies the presences of silver and zinc elements within the polyelectrolyte layers (marked with red dots). EDX analysis in mapping mode confirmed the good dispersion of the nanoparticles across the membrane surfaces, with only few unavoidable agglomerations [19]. The employment of negatively charged PSS as a dispersion medium for the nanoparticles was aimed at minimising the agglomerations. However, the strong ionic attractions between polycations and negatively charged nanoparticles inevitably induce the formation of larger agglomerates within the multi-layered system. This reduced the permeation of the nanoparticle agglomerates through the porous PES substrate.

Field emission scanning electron microscopy (FESEM) verified that the particle/agglomerate sizes were in the range of 40–50 and 100–170 nm for Ag_2O and ZnO nanoparticles, respectively. The estimated sizes are close to those obtained through the size distribution analysis, as discussed. The agglomeration of nanoparticles becomes one of the most significant limiting factors in the incorporation of nanoparticles into polymeric membranes, whether through blending or deposition methods, owing to surface interactions such as van der Waals forces, overlap of the electrical double layer, steric interaction of adsorbed polymer, and hydration forces [24].

3.3. *Analysis of the water permeability*

Membrane B displayed the highest water permeability, owing to its porous structure and high-molecular weight cut-off value, which has been estimated commercially (Table 1). The current work employed Membrane B as a porous substrate for the surface modification in order to produce membranes with a similar pure water flux to the commercial NF1 membrane. The water permeability for the modified membrane was lower, as displayed by Membrane C, owing to the increase in the total membrane resistance [25] and possible deposition of polyelectrolyte molecules within the pores of the porous membrane [26]. The permeability of Membrane C was similar to that of the commercial NF1 membrane (Membrane A), but it improved slightly in the presence of nanoparticles (Membrane D and Membrane E), owing to the formation of nanosized gaps around the nanoparticles from the poor compatibility of the inorganic nanoparticle surface and the polymer, which prevented the polymer chains from closely contacting the inorganic nanoparticles [27]. The formation of nanosized gaps increased the membrane porosity and encouraged the permeation of water molecules. However, this could contribute to the lower membrane retention capability, as seen from the salt retention results.

3.4. *Nanoparticle and polyelectrolyte leaching studies*

ICP analyses (Table 2) showed that neither Ag_2O nor ZnO were detected in the blank or permeated samples, which postulated that no nanoparticles had permeated through the polymeric membranes when pressure was applied. However, extremely low concentrations of Ag_2O and ZnO were detected (less than 1 ppm) in the retentate samples when employing Membrane D and Membrane E. This showed that the incorporation of nanoparticles into the polyelectrolyte multilayers minimised the leaching of the nanoparticles into the permeate streams. The formation of tight complexes between the polycations and polyanions successfully prevented the leaching of nanoparticles into the permeate streams during the filtration process. In addition, agglomerates formed between the negatively charged nanoparticles and polycations, which also helped to minimise the leaching through the membrane permeate stream. However, some of the formed aggregates on the membrane surface will contribute to a higher resistance in the fluid vortex, which possibly contributes to the formation of turbulence in the flow, thus contributing to the leaching of the aggregates from the membrane surface. Ways to improve the stability of nanoparticles that are

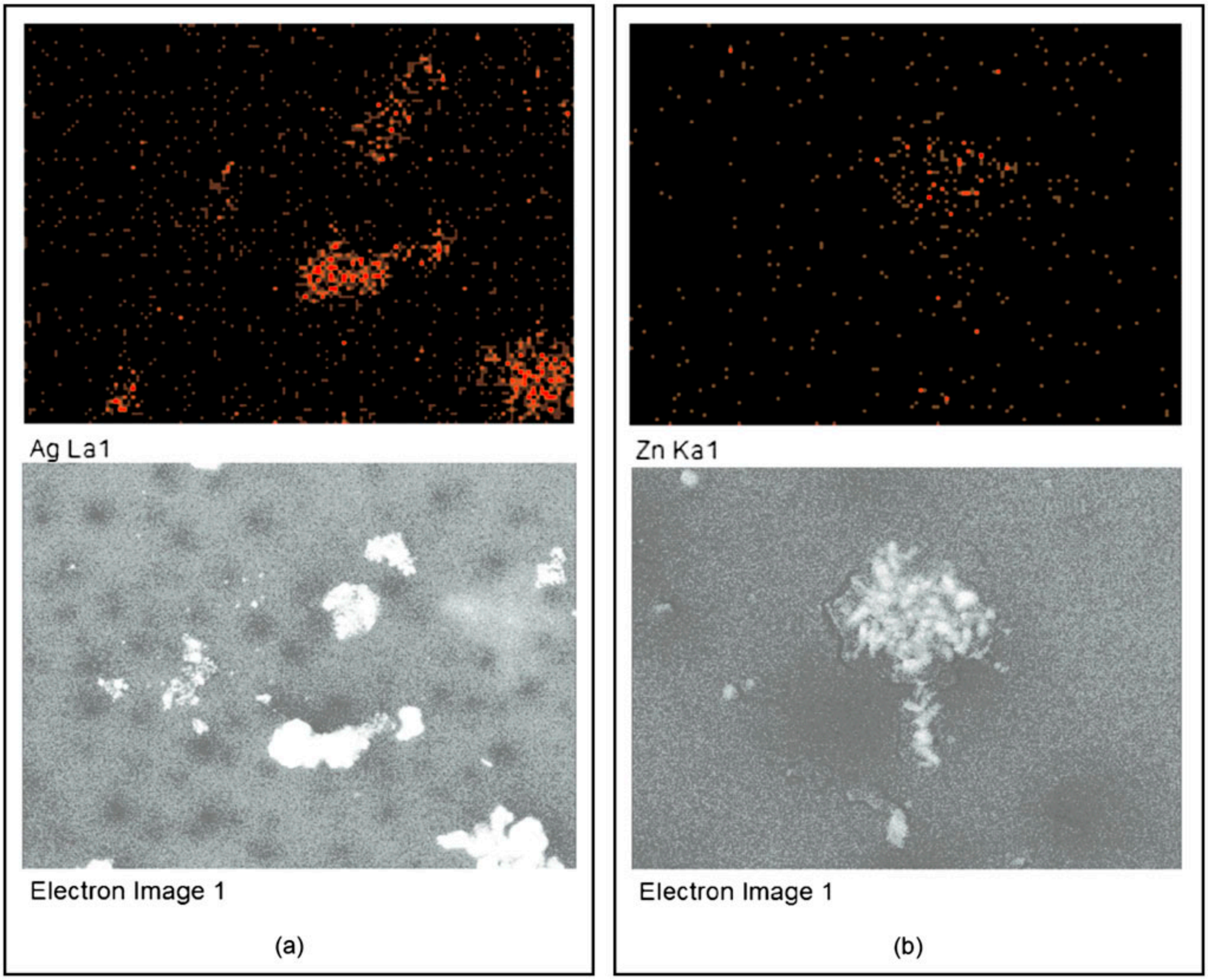

Fig. 2. EDX analysis conducted in mapping mode on (a) Membrane D and (b) Membrane E.

Table 2
Analysis of the samples collected during the water filtration processes using Membrane D and Membrane E

Sample label	Concentration (mg/L)	Description
Blank solutions		
Ag_2O	<0.01	Not detected
ZnO	<0.01	Not detected
Membrane D		
Retentate	0.02	Extremely low concentration of Ag_2O
Permeate	<0.01	Not detected
Membrane E		
Retentate	0.02	Extremely low concentration of ZnO
Permeate	<0.01	Not detected

incorporated within the polyelectrolyte multilayers on a membrane surface require further investigation in order to minimise the leaching of nanoparticles into feed samples. This is important to ensure that the modified membranes have consistent membrane performances for extended application durations.

As the stability of polyelectrolyte multilayers depends mostly on the charge density of the polyelectrolyte itself [28], a good film stability is expected when highly charged polyelectrolytes are employed. Standard curves of polycations and polyanions were obtained at wavelengths of 250 and 320 nm, respectively. Both curves displayed high linearity with regression greater than 0.99. A negligible amount of polyelectrolyte was confirmed to be present in permeate (<0.0005 wt%) and retentate (<0.0006 wt%) samples, which showed stable and good film formation properties. Employment of polyelectrolytes with large molecular weights (MWs) is also important in order to prevent the polyelectrolytes from passing through the polymeric substrate [29], which has been verified in this work. Large molecular weight polyelectrolytes demonstrated good pore-sealing characteristics and minimised the number of bilayers required to produce membranes with good retention capabilities.

3.5. Membrane retention capability

Membrane A typically showed high rejection towards all salt solutions, whereas the unmodified, commercial PES20 membrane (Membrane B) showed extremely low rejection towards all salt and humic acid solutions, owing to its porous structure (see Fig. 3). Deposition of polyelectrolyte multilayers improved the Na_2SO_4 salt rejection from 23.6 to 85.8% (Membrane C), making it about four times higher than the unmodified UF membrane (Membrane B), owing to the presence of excessive charges in the membrane separation layers, which enhanced the effective membrane repulsion capability towards the permeating ions [30]. Rejections between salt ions can also be attributed to differences in hydrated ion sizes or salvation energies [31]. However, in the presence of Ag_2O and ZnO nanoparticles (Membrane D and Membrane E), the salt-ion retention capability was slightly affected by the improved membrane porosity. Membranes with higher porosities will impose lower restrictions on the permeation of salt ions in addition to the water molecules. This can be verified through the improved water permeability but lower salt-ion retention capability that is observed (Membrane D and Membrane E) compared to the membrane modified using polyelectrolyte multilayers (Membrane C). Humic acid retention for Membrane B was improved by more than 10% when the membrane surfaces were modified through the deposition of polyelectrolyte multilayers, which is much better than previous work [32], owing to a better size exclusion mechanism. Incorporation of nanoparticles into the polyelectrolyte multilayers slightly reduced membrane retention towards humic acid (about 2%) because of the increased membrane porosity [12]. However, humic acid retention for all of the modified membranes was comparable to the commercial NF1 membrane, but the modified membranes showed lower restrictions to the passage of salt ions. This modification method offers the possibility to produce a NF membrane with a similar pure water flux and good retention towards large organic molecules, while exhibiting a lower tendency to be fouled by salt-ion scaling on the membrane surface. However, further investigation is required to prove this postulation.

Fig. 4 shows the selectivities of various salts over humic acid for each of the membranes. Membrane B showed no significant difference in selectivities for the various salts over humic acid. Membrane C, with polyelectrolyte multilayers, exhibited better selectivities for various salts over humic acid compared to the unmodified NF1 membrane (Membrane A), owing to better pore sealing and size exclusion effects [33,34]. The enhanced selectivities for polyelectrolyte-modified membranes, especially for the selectivities of NaCl/humic acid, could be a direct result of the increased charge density and thus electrostatic interactions [35] between the membrane surface and the solutes. Humic acid is known to be a negatively charged solute for most solution pH values [36]. Thus,

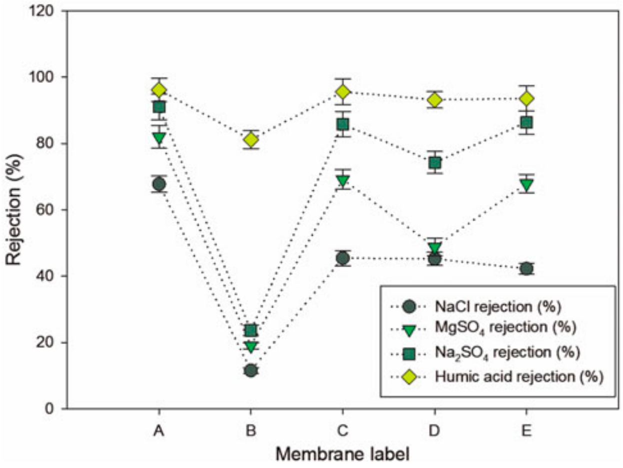

Fig. 3. Membrane rejection capabilities for various salts and humic acid.

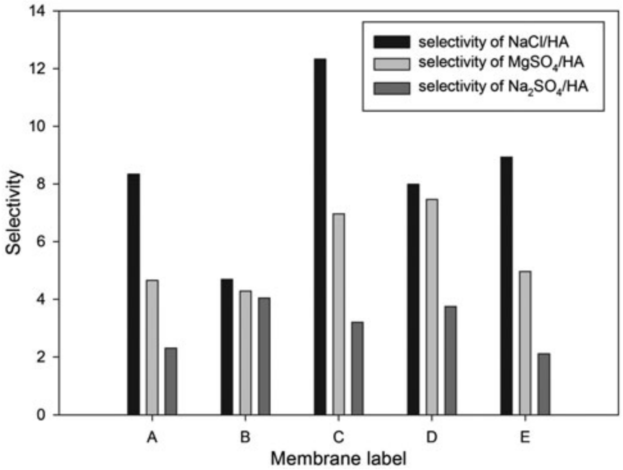

Fig. 4. Selectivities of various salts over humic acid.

deposition of the humic acid solutes onto the PSS layer on the surface of a modified membrane is minimised. This is in good agreement with the current observation.

High water permeability resulted in an increased deposition rate of the solutes onto the membrane surface during rejection testing. The higher permeation rate of water molecules encourages more humic acid

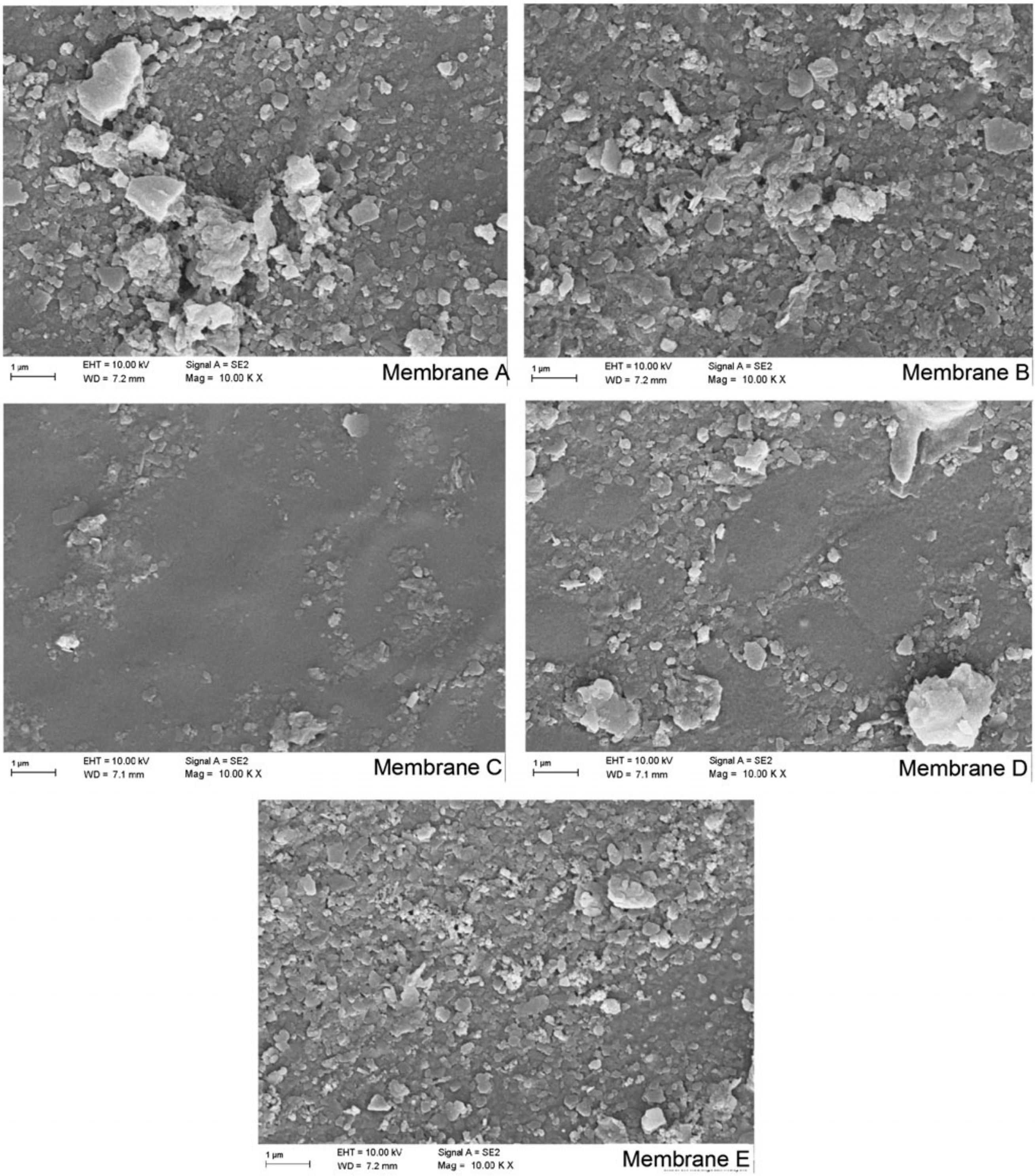

Fig. 5. Humic acid deposition onto the membrane surfaces, as visualised by FESEM.

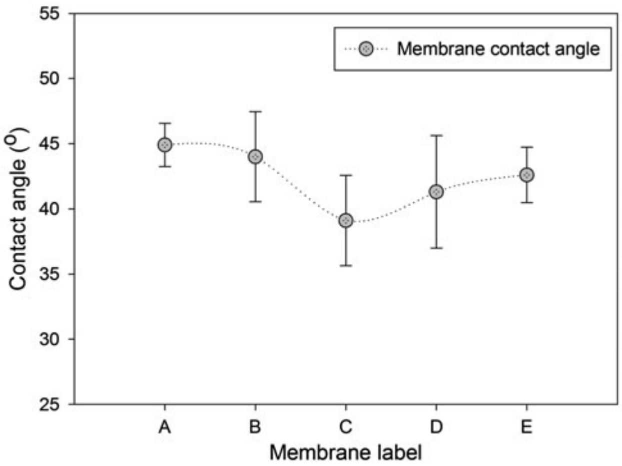

Fig. 6. Surface contact angles of modified and unmodified membranes.

solutes to come closer to the membrane surface pores. The pores of the membrane act as a separating barrier, hindering the solutes from passing through the membrane pores. This contributes to the higher deposition rate of humic acid solutes onto the membrane surface, as observed on Membrane B. Good control of the membrane surface characteristics is important in minimising the deposition of solutes. The formation of polyelectrolyte multilayers, preferably with a negatively charged surface, can possibly reduce the solute deposition phenomenon observed, owing to an improved repulsion capability [37]. In addition, lower water permeation through the pores of modified membranes also reduces the number of humic acid solutes that come closer to the membrane surfaces, which minimises the amount of humic acid solutes deposited onto the membrane surface. The membrane with polyelectrolyte layers (Membrane C) showed relatively stable fluxes with reduced deposition of humic acid onto the membrane surfaces (see Fig. 5). The lower surface contact angle after deposition of the PSS layer also minimised the deposition of humic acid particles onto the surface of the modified membrane (see Fig. 6), owing to improved surface wettability and self-cleaning effects [38]. Improved membrane surface wettability has been reported to minimise the adhesion of the solutes on the membrane surface [37].

4. Conclusion

In conclusion, the modified membranes in the current work showed a promising way to increase the retention capability of humic acid in water resources, while having better selectivity towards salt ions compared to the commercial NF membrane. This can extend the membrane lifespan by reducing membrane fouling, which is caused by salt-ion scaling. Incorporation of the nanoparticles within the polyelectrolyte multilayers improved the water permeability, while having humic acid retention similar to that of the commercial membrane (Membrane A). The polyelectrolyte-modified membrane showed decreased deposition of humic acid on the membrane surface, owing to the improved hydrophilicity and the Donnan effect. Based on these results, the polyelectrolyte-modified membranes in this study could be used in the pretreatment of potable water, in which the fractionation of the salt-ion mixture is desired, in addition to the partial removal of humic substances from water resources. Fewer humic acid molecules deposited onto the polyelectrolyte-modified membrane surface suggests that the current modification method can be used to develop a new kind of membrane with antifouling properties.

Acknowledgements

Financial supports from the following agencies are acknowledged: (i) Universiti Kebangsaan Malaysia through project DIP-2012-01 Research Grant Scheme and (ii) MOSTI through grant 03-01-02-SF0863.

List of symbols

C_f — feed solution concentration (ppm)
C_p — permeate solution concentration (ppm)
J — water or solution flux (L m^{-2} h^{-1})
R_{obs} — observed solute rejection (%)
S — surface area of membrane (m^2)
t — time interval (h^{-1})
V — volume of solution (L)

References

[1] C. Jarusutthirak, S. Mattaraj, R. Jiraratananon, Factors affecting nanofiltration performances in natural organic matter rejection and flux decline, Sep. Purif. Technol. 58 (2007) 68–75.
[2] J.D. Johnson, R.F. Christman, D.L. Norwood, D.S. Millington, Reaction products of aquatic humic substances with chlorine, Environ. Health Perspect. 46 (1982) 63–71.
[3] E.E. Chang, Y.-C. Chang, C.-H. Liang, C.-P. Huang, P.-C. Chiang, Identifying the rejection mechanism for nanofiltration membranes fouled by humic acid and calcium ions exemplified by acetaminophen, sulfamethoxazole, and triclosan, J. Hazard. Mater. 221–222 (2012) 19–27.

[4] T.M. Patel, K. Nath, Separation of ternary sodium chloride/reactive black-5 aqueous solutions using two different modules in a nanofiltration pilot plant, Int. J. Environ. Sci. Technol. 11 (2014) 1237–1248.
[5] K.-J. Kim, A.G. Fane, Performance evaluation of surface hydrophilized novel ultrafiltration membranes using aqueous proteins, J. Membr. Sci. 99 (1995) 149–162.
[6] G. Gosheger, J. Hardes, H. Ahrens, A. Streitburger, H. Buerger, M. Erren, A. Gunsel, F.H. Kemper, W. Winkelmann, C. von Eiff, Silver-coated megaendoprostheses in a rabbit model—An analysis of the infection rate and toxicological side effects, Biomaterials 25 (2004) 5547–5556.
[7] M.A. Hollinger, Toxicological aspects of topical silver pharmaceuticals, Crit. Rev. Toxicol. 26 (1996) 255–260.
[8] S. Nam, D. Parikh, B. Condon, Q. Zhao, M. Yoshioka-Tarver, Importance of poly(ethylene glycol) conformation for the synthesis of silver nanoparticles in aqueous solution, J. Nanopart. Res. 13 (2011) 3755–3764.
[9] T.-H. Bae, T.-M. Tak, Effect of TiO_2 nanoparticles on fouling mitigation of ultrafiltration membranes for activated sludge filtration, J. Membr. Sci. 249 (2005) 1–8.
[10] W. Chen, Y. Su, L. Zhang, Q. Shi, J. Peng, Z. Jiang, In situ generated silica nanoparticles as pore-forming agent for enhanced permeability of cellulose acetate membranes, J. Membr. Sci. 348 (2010) 75–83.
[11] L.-H. Li, J.-C. Deng, H.-R. Deng, Z.-L. Liu, L. Xin, Synthesis and characterization of chitosan/ZnO nanoparticle composite membranes, Carbohydr. Res. 345 (2010) 994–998.
[12] L.Y. Ng, A.W. Mohammad, C.P. Leo, N. Hilal, Polymeric membranes incorporated with metal/metal oxide nanoparticles: A comprehensive review, Desalination 308 (2013) 15–33.
[13] J. Kochan, M. Scheidle, J. van Erkel, M. Bikel, J. Büchs, J.E. Wong, T. Melin, M. Wessling, Characterization of antibacterial polyethersulfone membranes using the respiration activity monitoring system (RAMOS), Water Res. 46 (2012) 5401–5409.
[14] Y. Lvov, K. Ariga, M. Onda, I. Ichinose, T. Kunitake, Alternate assembly of ordered multilayers of SiO_2 and other nanoparticles and polyions, Langmuir 13 (1997) 6195–6203.
[15] L.Y. Ng, A.W. Mohammad, C.Y. Ng, N.H.H. Hairom, Stability and performance study of polyethersulfone membranes modified using polyelectrolytes, J. Teknol. 65 (2013) 7–12.
[16] L.Y. Ng, A.W. Mohammad, C.Y. Ng, C.P. Leo, R. Rohani, Development of nanofiltration membrane with high salt selectivity and performance stability using polyelectrolyte multilayers, Desalination 351 (2014) 19–26.
[17] L.Y. Ng, A.W. Mohammad, R. Rohani, C.Y. Ng, Optimization of polymeric membrane characteristics through thermal treatment and deposition of polyelectrolyte layers using response surface modeling, Adv. Polym. Technol. 34 (2014) 21472-1–21472-15.
[18] L.-Y. Yu, H.-M. Shen, Z.-L. Xu, PVDF-TiO_2 composite hollow fiber ultrafiltration membranes prepared by TiO_2 sol–gel method and blending method, J. Appl. Polym. Sci. 113 (2009) 1763–1772.
[19] L.Y. Ng, C.P. Leo, A.W. Mohammad, Optimizing the incorporation of silica nanoparticles in polysulfone/poly(vinyl alcohol) membranes with response surface methodology, J. Appl. Polym. Sci. 121 (2011) 1804–1814.
[20] P. Ahmadiannamini, X. Li, W. Goyens, B. Meesschaert, I.F.J. Vankelecom, Multilayered PEC nanofiltration membranes based on SPEEK/PDDA for anion separation, J. Membr. Sci. 360 (2010) 250–258.
[21] S. Lee, R.M. Lueptow, Reverse osmosis filtration for space mission wastewater: Membrane properties and operating conditions, J. Membr. Sci. 182 (2001) 77–90.
[22] J. Shao, J. Hou, H. Song, Comparison of humic acid rejection and flux decline during filtration with negatively charged and uncharged ultrafiltration membranes, Water Res. 45 (2011) 473–482.
[23] V.G. Pol, D.N. Srivastava, O. Palchik, V. Palchik, M.A. Slifkin, A.M. Weiss, A. Gedanken, Sonochemical deposition of silver nanoparticles on silica spheres, Langmuir 18 (2002) 3352–3357.
[24] J. Schaep, C. Vandecasteele, R. Leysen, W. Doyen, Salt retention of Zirfon® membranes, Sep. Purif. Technol. 14 (1998) 127–131.
[25] R. Malaisamy, A. Talla-Nwafo, K.L. Jones, Polyelectrolyte modification of nanofiltration membrane for selective removal of monovalent anions, Sep. Purif. Technol. 77 (2011) 367–374.
[26] R. Malaisamy, M.L. Bruening, High-flux nanofiltration membranes prepared by adsorption of multilayer polyelectrolyte membranes on polymeric supports, Langmuir 21 (2005) 10587–10592.
[27] H. Cong, M. Radosz, B.F. Towler, Y. Shen, Polymer–inorganic nanocomposite membranes for gas separation, Sep. Purif. Technol. 55 (2007) 281–291.
[28] N.G. Hoogeveen, M.A. Cohen Stuart, Formation and stability of multilayers of polyelectrolytes, Langmuir 12 (1996) 3675–3681.
[29] Z. Zhu, X. Feng, A. Penlidis, Self-assembled nano-structured polyelectrolyte composite membranes for pervaporation, Mater. Sci. Eng.: C 26 (2006) 1–8.
[30] L. Krasemann, B. Tieke, Selective ion transport across self-assembled alternating multilayers of cationic and anionic polyelectrolytes, Langmuir 16 (1999) 287–290.
[31] C. Cheng, A. Yaroshchuk, M.L. Bruening, Fundamentals of selective ion transport through multilayer polyelectrolyte membranes, Langmuir 29 (2013) 1885–1892.
[32] M.N. Abu Seman, M. Khayet, Z.I. Bin Ali, N. Hilal, Reduction of nanofiltration membrane fouling by UV-initiated graft polymerization technique, J. Membr. Sci. 355 (2010) 133–141.
[33] G. Ladam, P. Schaad, J.C. Voegel, P. Schaaf, G. Decher, F. Cuisinier, In situ determination of the structural properties of initially deposited polyelectrolyte multilayers, Langmuir 16 (1999) 1249–1255.

[34] M.D. Miller, M.L. Bruening, Controlling the nanofiltration properties of multilayer polyelectrolyte membranes through variation of film composition, Langmuir 20 (2004) 11545–11551.

[35] S. Saksena, A.L. Zydney, Effect of solution pH and ionic strength on the separation of albumin from immunoglobulins (IgG) by selective filtration, Biotechnol. Bioeng. 43 (1994) 960–968.

[36] A.E. Childress, M. Elimelech, Relating nanofiltration membrane performance to membrane charge (electrokinetic) characteristics, Environ. Sci. Technol. 34 (2000) 3710–3716.

[37] M. Zhang, B.-Q. Liao, X. Zhou, Y. He, H. Hong, H. Lin, J. Chen, Effects of hydrophilicity/hydrophobicity of membrane on membrane fouling in a submerged membrane bioreactor, Bioresour. Technol. 175 (2015) 59–67.

[38] J. Zhang, Q. Wang, Z. Wang, C. Zhu, Z. Wu, Modification of poly(vinylidene fluoride)/polyethersulfone blend membrane with polyvinyl alcohol for improving antifouling ability, J. Membr. Sci. 466 (2014) 293–301.